

Preparation and electrochemical magnesium insertion behaviors of $\text{Mg}_{0.5+y}(\text{Me}_y\text{Ti}_{1-y})_2(\text{PO}_4)_3$ ($\text{Me} = \text{Cr}, \text{Fe}$)

Koji Makino^{*}, Yasushi Katayama, Takashi Miura, Tomiya Kishi

Department of Applied Chemistry, Faculty of Science and Technology, Keio University,
Hiyoshi 3-14-1, Kohoku-ku, Yokohama 223-8522, Japan

Received 2 November 2001; received in revised form 6 March 2002; accepted 10 June 2002

Abstract

A series of transition metal phosphates, $\text{Mg}_{0.5+y}(\text{Fe}_y\text{Ti}_{1-y})_2(\text{PO}_4)_3$ (MFTP) and $\text{Mg}_{0.5+y}(\text{Cr}_y\text{Ti}_{1-y})_2(\text{PO}_4)_3$ (MCTP), modified from $\text{Mg}_{0.5}\text{Ti}_2(\text{PO}_4)_3$ (MTP) were prepared by sol–gel method and evaluated as a possible cathode material for magnesium cells. The lattice structures of MFTP and MCTP at $0 \leq y \leq 0.5$ were identical with that of MTP, while their unit cell volumes were smaller than that of MTP due to the increased amount of Mg^{2+} ions. Electrochemical magnesium insertion into MFTP and MCTP was found to be possible as observed for MTP. However, the limiting extent of magnesium insertion into MFTP at $0.1 \leq y \leq 0.5$ was small compared with MTP and remarkably dependent on the discharge current density during discharge. These facts suggested that the insertion limit is determined not by the number of available sites for Mg^{2+} or electrons but by the mobility of Mg^{2+} in these host materials correlating with decrease in the unit cell volume. © 2002 Elsevier Science B.V. All rights reserved.

Keywords: Magnesium battery; Magnesium titanium phosphate; Electrochemical magnesium insertion

1. Introduction

Electrochemical intercalation of multivalent cation instead of monovalent Li^+ or Na^+ has attracted much attention as a positive electrode reaction in secondary cells because of the expected large electrochemical equivalence. Particularly, recent interests are focused on Mg^{2+} , smaller than, more abundant than and less dangerous than lithium. One of the encountered difficulties is the low mobility of Mg^{2+} in the host lattice, since Mg^{2+} has high surface charge density [1–5]. Consequently, fast Mg^{2+} transport in the intercalation host is required at ambient temperature, which may be realized in a transition metal phosphate $\text{Mg}_{0.5+y}(\text{Me}_y\text{Ti}_{1-y})_2(\text{PO}_4)_3$ ($\text{Me} = \text{Cr}, \text{Fe}$). Those are derived from $\text{Mg}_{0.5}\text{Ti}_2(\text{PO}_4)_3$ (MTP) [6] and having the isostructural lattice with the so-called super ionic conductor of NASICON [7,8] proposed as a conductive solid electrolyte [9–11].

Since $\text{LiTi}_2(\text{PO}_4)_3$ was reported as an appropriate Li^+ insertion host by Delmas and Nadiri [12], various NASICON compounds have been investigated as a possible cathode

material. Both good high-rate performance and long cycling stability could be simultaneously expected for such materials, because they have large enough interstitial voids to accommodate guest cation and the stable lattice based on the three-dimensional framework [13–15].

In previous studies, magnesium could be inserted electrochemically into a titanium compound of $\text{Mg}_{0.5}\text{Ti}_2(\text{PO}_4)_3$ up to one Mg^{2+} per unit formula [16]. Moreover, the insertion limit might be determined not by the number of available sites for Mg^{2+} but by that of electrons [17].

In the present work, the effects of partial substitution of Ti^{4+} in the $\text{Mg}_{0.5}\text{Ti}_2(\text{PO}_4)_3$ lattice with foreign trivalent transition metal cation of Fe^{3+} or Cr^{3+} on the electrochemical Mg^{2+} insertion behaviors have been investigated in a propylene carbonate solution to compare with previous data [16,17].

2. Experimental

2.1. Preparation of $\text{Mg}_{0.5+y}(\text{Me}_y\text{Ti}_{1-y})_2(\text{PO}_4)_3$ ($\text{Me} = \text{Cr}, \text{Fe}$)

$\text{Mg}(\text{CH}_3\text{COO})_2 \cdot 4\text{H}_2\text{O}$ (0.1 mol dm^{-3}) (Wako Chemical, >99%) and 0.1 mol dm^{-3} $\text{NH}_4\text{H}_2\text{PO}_4$ (Wako Chemical,

^{*} Corresponding author. Tel.: +81-45-566-1561; fax: +81-45-566-1561.
E-mail address: c08726@edu.cc.keio.ac.jp (K. Makino).

>99%) aqueous solutions were prepared separately, in addition to 0.1 mol dm^{-3} $\text{C}_4\text{H}_9\text{O}[\text{Ti}(\text{OC}_4\text{H}_9)_2\text{O}]_4\text{C}_4\text{H}_9$ (Wako Chemical, >95%) and 0.1 mol dm^{-3} $\text{CrCl}_3 \cdot 6\text{H}_2\text{O}$ (Wako Chemical, >98%) or FeCl_3 (Wako Chemical, >95%) ethanol solution. These solutions were mixed at a desirable ratio to give a certain y -value in $\text{Mg}_{0.5+y}(\text{Me}_y\text{Ti}_{1-y})_2(\text{PO}_4)_3$. The obtained sol solution was further stirred at 70°C for 6 h to form a gel, which was then dried at 90°C for 12 h. This powder was heated at 300°C and then at 500°C to remove ammonium and acetate groups, followed by final firing at various temperatures for 24 h.

2.2. Electrochemical measurements

Electrochemical magnesium insertion from 1 mol dm^{-3} $\text{Mg}(\text{ClO}_4)_2$ /propylene carbonate (PC) solution was performed in a cylindrical glass cell. The sample electrode pellet was prepared by pressing the 70:25:5 (w/w/w) mixture of $\text{Mg}_{0.5+y}(\text{Me}_y\text{Ti}_{1-y})_2(\text{PO}_4)_3$, acetylene black (Denka Black, Denkikagaku Kogyo) and PTFE (Mitsui-Du Pont) at a pressure of $2 \times 10^3 \text{ kg cm}^{-2}$ onto a porous nickel sheet. Magnesium ribbon was used as the counter electrode. The reference electrode consisted of a silver wire immersed in 0.1 mol dm^{-3} AgClO_4 /PC solution, which was separated from the cell electrolyte by a glass filter. All procedures and cell construction were carried out under dried argon atmosphere in a glove box.

X-ray diffraction (XRD, Rigaku, RINT-1300) measurements were performed on a nickel substrate using an aluminum folder both before and after electrochemical measurements as well as for prepared MTP, $\text{Mg}_{0.5+y}(\text{Fe}_y\text{Ti}_{1-y})_2(\text{PO}_4)_3$ (MFTP) and $\text{Mg}_{0.5+y}(\text{Cr}_y\text{Ti}_{1-y})_2(\text{PO}_4)_3$ (MCTP) powder on a glass plate.

3. Results and discussion

3.1. Preparation of $\text{Mg}_{0.5+y}(\text{Me}_y\text{Ti}_{1-y})_2(\text{PO}_4)_3$ ($\text{Me} = \text{Cr}, \text{Fe}$)

The MFTP samples, having the y -value of 0.5 in $\text{Mg}_{0.5+y}(\text{Fe}_y\text{Ti}_{1-y})_2(\text{PO}_4)_3$ (MFTP) and prepared at various final firing temperatures (T_F), were investigated by XRD measurements (Fig. 1) in order to optimize T_F . When T_F was set below 500°C , the sample was apparently amorphous. The crystalline MFTP phase could be obtained at $T_F = 700^\circ\text{C}$ and all diffraction lines were consistent with the simulation data as hexagonal (space group; $R\bar{3}c$). However, TiP_2O_7 and unknown impurity phases appeared at $T_F = 900^\circ\text{C}$ due to the decomposition of MFTP.

The XRD patterns of various samples, obtained at $T_F = 700^\circ\text{C}$ and having different nominal compositions in $0 \leq y \leq 1.0$, were compared in Fig. 2. MFTP having the same lattice structure as MTP could be obtained as single phase only at $0 \leq y \leq 0.5$ without any uncertain XRD line. $\text{Mg}_3(\text{PO}_4)_2$ and FePO_4 phases appeared at $0.5 < y$. The peak

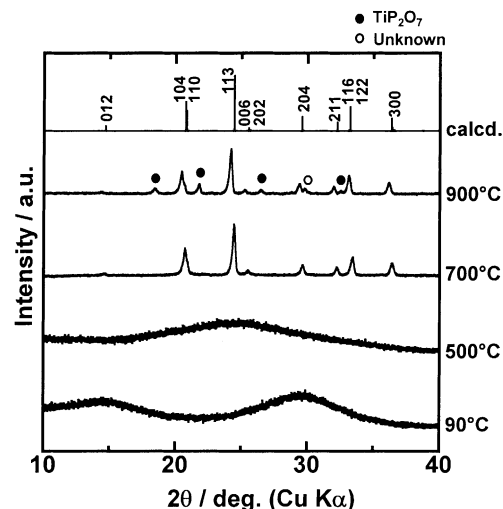


Fig. 1. XRD patterns of $\text{Mg}_{1.0}(\text{Fe}_{0.5}\text{Ti}_{0.5})_2(\text{PO}_4)_3$ obtained at various temperatures. Simulation; space group $R\bar{3}c$, $a = 8.55 \text{ \AA}$, $c = 20.8 \text{ \AA}$.

intensities of such impurities increased with increasing y . These results suggest that solid solution region of MFTP phases lies at $0 \leq y \leq 0.5$.

Similarly, MCTP samples having nominal composition of $0 \leq y \leq 1.0$ in $\text{Mg}_{0.5+y}(\text{Cr}_y\text{Ti}_{1-y})_2(\text{PO}_4)_3$ and fired at $T_F = 700^\circ\text{C}$ were investigated by XRD measurements (Fig. 3). MCTP obtained only at $0 \leq y \leq 0.5$ is hexagonal and belongs to the space group $R\bar{3}c$ like as MTP. At $0.5 < y$ some unidentified weak XRD lines appeared.

The effects of Ti^{4+} substitution with Fe^{3+} or Cr^{3+} on lattice parameters were summarized in Fig. 4, where the shrinkage in c -axis occurs due both to the relaxed O–O repulsion in $(\text{Me}, \text{Ti})\text{O}_6$ octahedra and to the bond formation

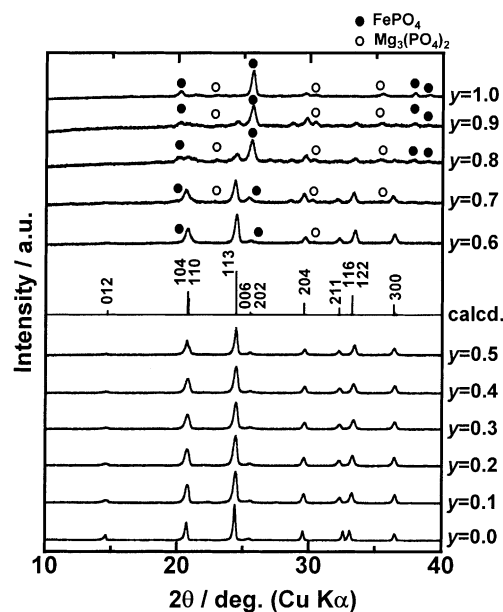


Fig. 2. XRD patterns of $\text{Mg}_{0.5+y}(\text{Fe}_y\text{Ti}_{1-y})_2(\text{PO}_4)_3$ ($y = 0-1.0$) obtained at 700°C . Simulation; space group $R\bar{3}c$, $a = 8.55 \text{ \AA}$, $c = 20.8 \text{ \AA}$.

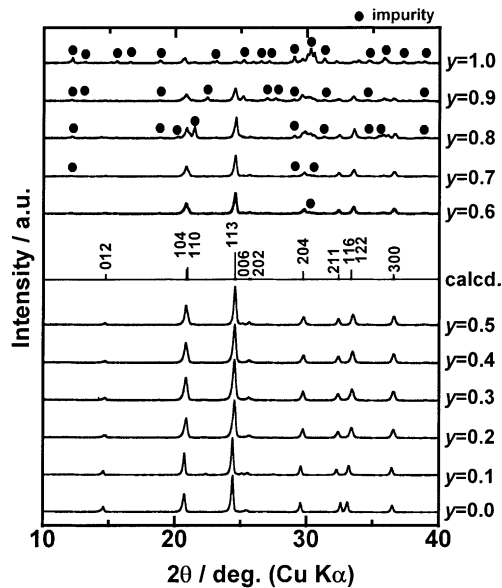


Fig. 3. XRD patterns of $\text{Mg}_{0.5+y}(\text{Cr}_y\text{Ti}_{1-y})_2(\text{PO}_4)_3$ ($y = 0-1.0$) obtained at 700°C . Simulation; space group $R\bar{3}c$, $a = 8.54 \text{ \AA}$, $c = 20.7 \text{ \AA}$.

between introduced excess Mg^{2+} and O in $(\text{Me}, \text{Ti})\text{O}_6$ octahedra. On the other hand, a -axis expands to compensate the c -shrinkage in the flexible NASICON framework having a certain degree of freedom, because $(\text{Me}, \text{Ti})\text{O}_6$ octahedra share corners with PO_4 tetrahedra [18]. However, this compensation seems too little to prevent the decrease in unit cell volume. The unit cell volume of both MFTP and MCTP decreases remarkably at $0 \leq y \leq 0.1$ then gradually at $0.1 \leq y \leq 0.5$. The different tendency of unit cell parameter changes between MFTP and MCTP seems to arise from the difference of ionic radius between Fe^{3+} (0.67 \AA) and Cr^{3+} (0.64 \AA) in octahedra [19].

3.2. Electrochemical magnesium insertion

All the electrochemical magnesium insertion experiments were performed for the samples obtained at $T_F = 700^\circ\text{C}$.

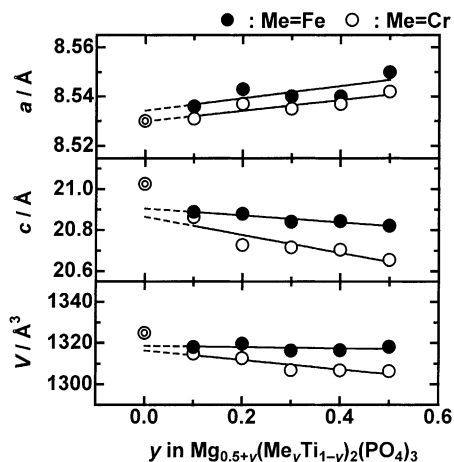


Fig. 4. Unit cell parameters of $\text{Mg}_{0.5+y}(\text{Me}_y\text{Ti}_{1-y})_2(\text{PO}_4)_3$.

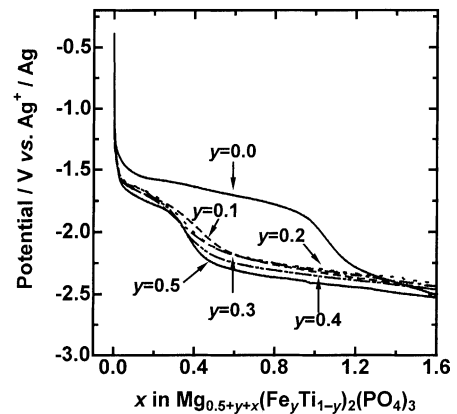


Fig. 5. Galvanostatic ($-50 \mu\text{A cm}^{-2}$) discharge curves of $\text{Mg}_{0.5+y}(\text{Fe}_y\text{Ti}_{1-y})_2(\text{PO}_4)_3$.

Galvanostatic discharge curves ($-50 \mu\text{A cm}^{-2}$ based on apparent geometrical area) of MFTP ($y = 0.1-0.5$) and MTP were compared in Fig. 5 in order to confirm the effect of substitution of Ti^{4+} with Fe^{3+} . For MTP the potential plateau at about -1.6 V (versus Ag^+/Ag) continues until the limit of electronic accommodation by $\text{Ti}^{4+}/\text{Ti}^{3+}$ (reduction of Ti^{4+} to Ti^{3+}) defined as $x = 1.0$, where x denotes the calculated amount of inserted Mg^{2+} per formulae. As Mg dissolution on anodes occur at -2.20 V (versus Ag^+/Ag), Mg cell would be operated at ca. 0.5 V .

For MFTP ($y = 0.1-0.5$) similar plateau can be observed, although capacities are $x < 0.5$ and independent of y . At the final stage of $1.2 \leq x$, both MFTP and MTP show substantially identical discharge potential below -2.4 V , where an unexpected reaction such as the solvent decomposition might occur.

Effects of current densities on discharge curves of MFTP ($y = 0.1$ and 0.5), MCTP ($y = 0.5$) and MTP are shown in Fig. 6, where both the potential and capacities are rate-dependent markedly for MFTP ($y = 0.1$ and 0.5) and MCTP ($y = 0.5$) compared with MTP owing to the low mobility of Mg^{2+} in the host lattice. Moreover, in order to confirm the

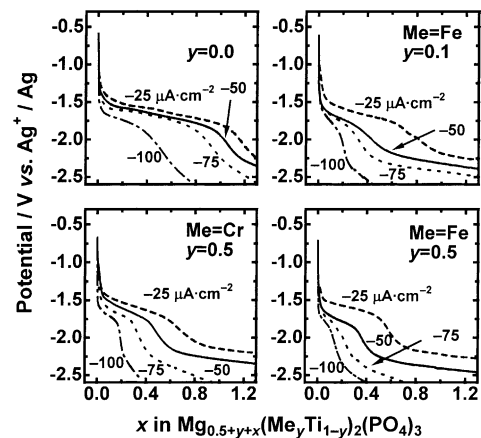


Fig. 6. Discharge curves of $\text{Mg}_{0.5+y}(\text{Me}_y\text{Ti}_{1-y})_2(\text{PO}_4)_3$ at various current densities.

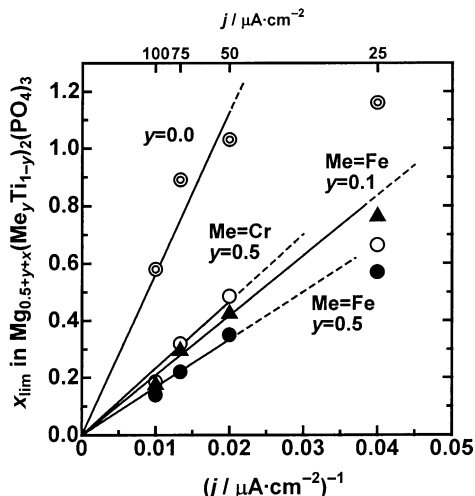


Fig. 7. Relationship between the limit of Mg insertion x_{lim} in $Mg_{0.5+y}(Me_yTi_{1-y})_2(PO_4)_3$ and current density.

diffusion controlled situation in the host matrix, the proportional relationship between the limiting amount of Mg insertion (x_{lim}), which corresponds to the plateau length until about -2.2 V and was determined from the inflection point of discharge curves at various current densities (j), and the inverse of j , (applying at $j \geq |-50 \mu A cm^{-2}|$) is examined for all the sample of MFTP ($y = 0.1$ and 0.5), MCTP ($y = 0.5$) and MTP, as seen Fig. 7. These results suggest that the insertion limit is controlled by the diffusion process and that MTP has better high-rate performance than MFTP or MCTP probably because of its large unit cell volume.

The XRD study during electrochemical Mg insertion ensured that magnesium insertion can proceed topotactically into all of MFTP ($y = 0.5$), MCTP ($y = 0.5$) and MTP as seen in Figs. 8–10, respectively, moreover the unit cell parameters at various stages of Mg insertion were summarized in Fig. 11. No any new XRD line appears after Mg insertion, where the unit cell parameters remain almost

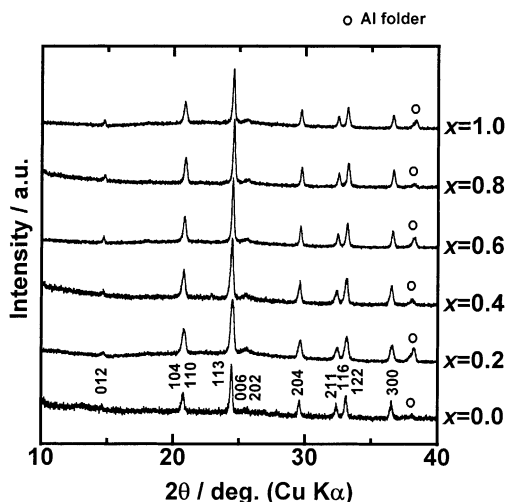


Fig. 8. XRD patterns of Mg inserted $Mg_{0.5+x}Ti_2(PO_4)_3$.

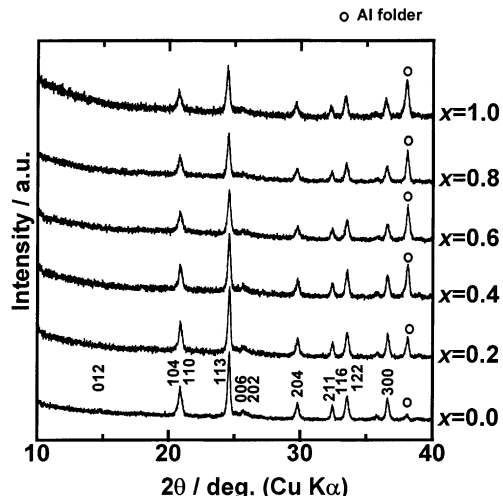


Fig. 9. XRD patterns of Mg inserted $Mg_{1.0+x}(Cr_{0.5}Ti_{0.5})_2(PO_4)_3$.

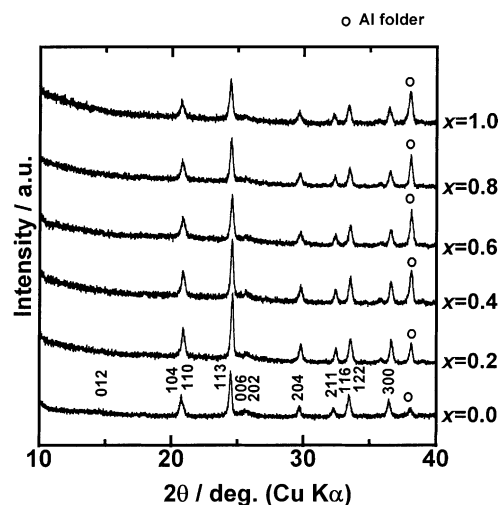


Fig. 10. XRD patterns of Mg inserted $Mg_{1.0+x}(Fe_{0.5}Ti_{0.5})_2(PO_4)_3$.

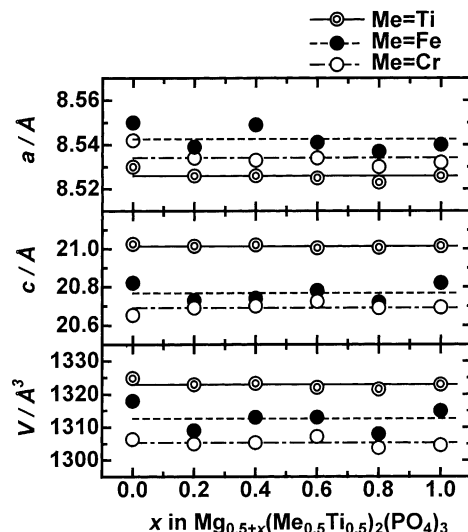


Fig. 11. Unit cell parameters at various stages of Mg insertion.

constant at various stages of magnesium insertion up to $x = 1.0$. Possibly, Mg^{2+} might be accommodated in these hosts like as a transparent guest, because NASICON-lattice has large cationic sites and the flexible structure.

4. Conclusion

MFTP and MCTP samples having MTP-lattice could be synthesized at $0 \leq y \leq 0.5$, and their unit cell volume was smaller than that of MTP owing to the c -shrinkage caused by introduced Mg^{2+} ions. Electrochemical magnesium insertion into MFTP and MCTP was found possible as into MTP. However, the insertion limits were smaller for MFTP and MCTP than $x = 1.0$ for MTP and decreased with increasing the discharge rate, suggesting that the insertion is still under kinetic control of Mg^{2+} diffusion in the hosts.

References

- [1] P. Novák, W. Scheifele, O. Haas, J. Power Sources 54 (1995) 479.
- [2] T.D. Gregory, R.J. Hoffman, R.C. Winterton, J. Electrochem. Soc. 137 (1990) 775.
- [3] M.E. Spahr, P. Novák, O. Haas, R. Nesper, J. Power Sources 54 (1995) 346.
- [4] P. Novák, W. Scheifele, F. Joho, O. Haas, J. Electrochem. Soc. 142 (1995) 2544.
- [5] P. Novák, J. Desilvestro, J. Electrochem. Soc. 140 (1993) 140.
- [6] S. Barth, R. Olazcuaga, P. Gravereau, G. Le Flem, P. Hagenmuller, Mater. Lett. 16 (1993) 96.
- [7] H.Y.-P. Hong, Mater. Res. Bull. 11 (1976) 173.
- [8] J.B. Goodenough, H.Y.-P. Hong, J.A. Kafalas, Mater. Res. Bull. 11 (1976) 203.
- [9] K. Nomura, S. Ikeda, K. Ito, H. Einaga, J. Electroanal. Chem. 326 (1992) 351.
- [10] K. Nomura, S. Ikeda, K. Ito, H. Einaga, Bull. Chem. Soc. Jpn. 65 (1992) 3221.
- [11] O. Mentre, F. Abraham, B. Deffontaines, P. Vast, Solid State Ionics 72 (1994) 293.
- [12] C. Delmas, A. Nadiri, Solid State Ionics 28 (1988) 419.
- [13] A.K. Padhi, K.S. Nanjundaswamy, C. Masquelier, J.B. Goodenough, J. Electrochem. Soc. 144 (1997) 2581.
- [14] K.S. Nanjundaswamy, A.K. Padhi, J.B. Goodenough, S. Okada, H. Ohtsuka, H. Arai, J. Yamaki, Solid State Ionics 92 (1996) 1.
- [15] A. Nadiri, C. Delmas, R. Salmon, P. Hagenmuller, Revue de Chimie Minérale 21 (1984) 537.
- [16] K. Makino, Y. Katayama, T. Miura, T. Kishi, J. Power Sources 99 (2001) 66.
- [17] K. Makino, Y. Katayama, T. Miura, T. Kishi, J. Power Sources 97 (2001) 512.
- [18] J. Alamo, Solid State Ionics 63–65 (1993) 547.
- [19] A.B. Bykov, A.P. Chirkin, L.N. Demyanets, S.N. Doronin, E.A. Genkina, A.K. Ivanov-Shits, I.P. Kondratyuk, B.A. Maksimov, L.N. Muradyan, V.I. Simonov, V.A. Timofeeva, Solid State Ionics 38 (1990) 31.